Development and Evaluation of Non-Reflective Boundary Conditions for Lattice Boltzmann Method

Fabien Chevillotte, Denis Ricot

fabien.chevillotte@matelys.com

AIAA 2016, Lyon, France

Mai 31st, 2016

22nd AIAA/CEAS Aeroacoustics Conference
Lyon, France – 30 May – 1 June, 2016

Introduction

- Non-reflective boundary conditions are of great interest in aeroacoustic simulations to avoid spurious reflections.
- Indeed, reflections could biais any acoustic assessment.
- Non-reflective boundary conditions allow to reduce the size of the domain and the computation cost.

Introduction

- Non-reflective boundary conditions are of great interest in aeroacoustic simulations to avoid spurious reflections.
- Indeed, reflections could biais any acoustic assessment.
- Non-reflective boundary conditions allow to reduce the size of the domain and the computation cost.

Introduction

- Non-reflective boundary conditions are of great interest in aeroacoustic simulations to avoid spurious reflections.
- Indeed, reflections could biais any acoustic assessment.
- Non-reflective boundary conditions allow to reduce the size of the domain and the computation cost.

Introduction

- Several types of non-reflective boundary conditions have been studied :
  - Characteristic boundary conditions (CBC),
  - Asymptotic far-field solutions,
  - Buffer zones techniques,
  - Perfectly match layers (PML),
  - Zonal CBC,
  - Transverse CBC (TCBC) and zonal TCBC.
- These methods have been studied in various simulation frameworks :
  - Linearized Euler Equations (LEE),
  - Navier-Stokes equations (NS),
  - Lattice Boltzmann method (LBM).

Introduction

- Several types of non-reflective boundary conditions have been studied :
  - Characteristic boundary conditions (CBC),
  - Asymptotic far-field solutions,
  - Buffer zones techniques,
  - Perfectly match layers (PML),
  - Zonal CBC,
  - Transverse CBC (TCBC) and zonal TCBC.
- These methods have been studied in various simulation frameworks :
  - Linearized Euler Equations (LEE),
  - Navier-Stokes equations (NS),
  - Lattice Boltzmann method (LBM).

Introduction

- On the other side, acoustical surface impedance model have been investigated in the time-domain.
- This study focuses on the **buffer zone damping** method and the **acoustical surface impedance** method in a lattice Boltzmann framework.

Introduction

- On the other side, acoustical surface impedance model have been investigated in the time-domain.
- This study focuses on the **buffer zone damping** method and the **acoustical surface impedance** method in a lattice Boltzmann framework.

Description of LBM solver

- The lattice Boltzmann solver LaBS has been employed.
- LaBS is built upon a classical D3Q19 lattice with two-relaxation time collision model.
- Turbulence is handled according LES approach.
- The dissipation and dispersion are kept as low as possible to enable proper generation & propagation of acoustic waves.

Description of LBM solver

- The lattice Boltzmann solver LaBS has been employed.
- LaBS is built upon a classical D3Q19 lattice with two-relaxation time collision model.
- Turbulence is handled according LES approach.
- The dissipation and dispersion are kept as low as possible to enable proper generation & propagation of acoustic waves.

Description of LBM solver

- The lattice Boltzmann solver LaBS has been employed.
- LaBS is built upon a classical D3Q19 lattice with two-relaxation time collision model.
- Turbulence is handled according LES approach.
- The dissipation and dispersion are kept as low as possible to enable proper generation & propagation of acoustic waves.

Description of LBM solver

- The lattice Boltzmann solver LaBS has been employed.
- LaBS is built upon a classical D3Q19 lattice with two-relaxation time collision model.
- Turbulence is handled according LES approach.
- The dissipation and dispersion are kept as low as possible to enable proper generation & propagation of acoustic waves.

Buffer zone technique

Using explicit buffer zone techniques, the damped solution field $\widetilde{U}^{i+1}$ writes at each time-step :

$$\widetilde{U}^{i+1} = U^{i+1} - \sigma(x)\left(U^{i+1} - U_{target}\right)$$

with $\sigma(x)$ the damping factor :

$$\sigma(x) = A\left(1 - \frac{L-x}{L-x_0}\right)^n$$

or

$$\sigma(x) = A\frac{(x-x_0)^n(L-x)(n+1)(n+2)}{(L-x_0)^{n+2}}$$

where x is the position along the damping layer, L its length and x_0 the starting position.

(Ref : Israeli 1981, Richards 2004, Gill 2015)

Buffer zone technique

Using explicit buffer zone techniques, the damped solution field $\widetilde{U}^{i+1}$ writes at each time-step :

$$\widetilde{U}^{i+1} = U^{i+1} - \sigma(x)\left(U^{i+1} - U_{target}\right)$$

with $\sigma(x)$ the damping factor :

$$\sigma(x) = A\left(1 - \frac{L-x}{L-x_0}\right)^n$$

or

$$\sigma(x) = A\frac{(x-x_0)^n(L-x)(n+1)(n+2)}{(L-x_0)^{n+2}}$$

where x is the position along the damping layer, L its length and x_0 the starting position.

(Ref : Israeli 1981, Richards 2004, Gill 2015)

Acoustical surface impedance

The surface impedance model proposed by Özyörük is an assembly of a low-pass, a pass-band and a high-pass filters and requires 7 coefficients z_i in the frequency domain.

$$\frac{Z(\omega)}{\rho_0 c_0} = z_1 + \frac{z_2 - z_1}{1 + i\omega z_3} + \frac{i\omega z_4}{\left(1 - \omega^2/z_6^2\right) + i\omega z_5} + i\omega z_7$$

The corresponding impedance model in the z-domain writes :

$$Z(z) = \frac{\sum_{l=0}^{4} a_l z^{-l}}{-\sum_{k=0}^{3} b_k z^{-k}}.$$

The coefficients a_i et b_i are identified from the z_i coefficients and the time step dt.

Acoustical surface impedance

The surface impedance model proposed by Özyörük is an assembly of a low-pass, a pass-band and a high-pass filters and requires 7 coefficients z_i in the frequency domain.

$$\frac{Z(\omega)}{\rho_0 c_0} = z_1 + \frac{z_2 - z_1}{1 + i\omega z_3} + \frac{i\omega z_4}{\left(1 - \omega^2/z_6^2\right) + i\omega z_5} + i\omega z_7$$

The corresponding impedance model in the z-domain writes :

$$Z(z) = \frac{\sum_{l=0}^{4} a_l z^{-l}}{-\sum_{k=0}^{3} b_k z^{-k}}.$$

The coefficients a_i et b_i are identified from the z_i coefficients and the time step dt.

Acoustical surface impedance

The impedance condition can be written at time $i + 1$:

$$a_0 v^{i+1} - c_0^2 \rho^{i+1} = c_0^2 \sum_{k=0}^{3} (b_k - b_{k+1}) \left(\rho^{i-k} - \rho_0\right) + \sum_{l=0}^{4} (a_l - a_{l+1})\, v^{i-l} - c_0^2 \rho_0$$

with v the normal velocity **relative to the mean flow**, ρ the density, ρ_0 the density of air and c_0 the speed of sound.

Non-reflective boundary condition with non-uniform flow

- The explicit buffer zone technique is known to **provide relatively good results if the target field** U_{target} (velocity and density) is **known**.
- Unfortunately for most of the realistic cases, the target outlet density is known $\rho_{target} = \rho_0$ but the target velocity field is not necessarily known.
- A solution would be to calculate the mean flow field $\overline{U^{i+1}}$ by using a **moving average** and to set as the target.
- Unfortunately, this solution is memory consuming when implemented in a straightforward manner.

Non-reflective boundary condition with non-uniform flow

- The explicit buffer zone technique is known to **provide relatively good results if the target field** U_{target} (velocity and density) is **known**.
- Unfortunately for most of the realistic cases, the target outlet density is known $\rho_{target} = \rho_0$ but the target velocity field is not necessarily known.
- A solution would be to calculate the mean flow field $\overline{U^{i+1}}$ by using a **moving average** and to set as the target.
- Unfortunately, this solution is memory consuming when implemented in a straightforward manner.

Non-reflective boundary condition with non-uniform flow

- The explicit buffer zone technique is known to **provide relatively good results if the target field** U_{target} (velocity and density) is **known**.
- Unfortunately for most of the realistic cases, the target outlet density is known $\rho_{target} = \rho_0$ but the target velocity field is not necessarily known.
- A solution would be to calculate the mean flow field $\overline{U^{i+1}}$ by using a **moving average** and to set as the target.
- Unfortunately, this solution is memory consuming when implemented in a straightforward manner.

Non-reflective boundary condition with non-uniform flow

- The explicit buffer zone technique is known to **provide relatively good results if the target field** U_{target} (velocity and density) is **known**.
- Unfortunately for most of the realistic cases, the target outlet density is known $\rho_{target} = \rho_0$ but the target velocity field is not necessarily known.
- A solution would be to calculate the mean flow field $\overline{U^{i+1}}$ by using a **moving average** and to set as the target.
- Unfortunately, this solution is memory consuming when implemented in a straightforward manner.

Non-reflective boundary condition with non-uniform flow

- Another way to estimate the moving average field is to use an accumulator :

  $$\overline{U^{i+1}} = (1 - C)\overline{U^i} + CU^{i+1}$$

  with C a very small value ($C < 0.01$).

- An accumulator is an integrator filter (low-pass filter) and decreasing C is equivalent to increase the integration time τ.
- C can be expressed as a low-pass filter $C = 1 - \mathrm{e}^{-t/\tau}$.

$$\overline{U^{i+1}} = \mathrm{e}^{-dt/\tau}\overline{U^i} + \left(1 - \mathrm{e}^{-dt/\tau}\right)U^{i+1} \quad (1)$$

Non-reflective boundary condition with non-uniform flow

- Another way to estimate the moving average field is to use an accumulator :
$$\overline{U^{i+1}} = (1 - C)\overline{U^i} + CU^{i+1}$$
with C a very small value ($C < 0.01$).
- An accumulator is an integrator filter (low-pass filter) and decreasing C is equivalent to increase the integration time τ.
- C can be expressed as a low-pass filter $C = 1 - e^{-t/\tau}$.

$$\overline{U^{i+1}} = e^{-dt/\tau}\overline{U^i} + \left(1 - e^{-dt/\tau}\right) U^{i+1} \quad (1)$$

Non-reflective boundary condition with non-uniform flow

- Another way to estimate the moving average field is to use an accumulator :
$$\overline{U^{i+1}} = (1 - C)\overline{U^i} + CU^{i+1}$$
with C a very small value ($C < 0.01$).
- An accumulator is an integrator filter (low-pass filter) and decreasing C is equivalent to increase the integration time τ.
- C can be expressed as a low-pass filter $C = 1 - \mathrm{e}^{-t/\tau}$.

$$\overline{U^{i+1}} = \mathrm{e}^{-dt/\tau}\overline{U^i} + \left(1 - \mathrm{e}^{-dt/\tau}\right) U^{i+1} \qquad (1)$$

Non-reflective boundary condition with non-uniform flow

- When unknown, the target field is dynamically evaluated with such a simple accumulator.
- This methodology can be used for the explicit buffer zone as well for the surface impedance method with an outgoing mean flow.
- This method will be called the **dynamic method**.

Non-reflective boundary condition with non-uniform flow

- When unknown, the target field is dynamically evaluated with such a simple accumulator.
- This methodology can be used for the explicit buffer zone as well for the surface impedance method with an outgoing mean flow.
- This method will be called the **dynamic method**.

Non-reflective boundary condition with non-uniform flow

- When unknown, the target field is dynamically evaluated with such a simple accumulator.
- This methodology can be used for the explicit buffer zone as well for the surface impedance method with an outgoing mean flow.
- This method will be called the **dynamic method**.

Usual test case

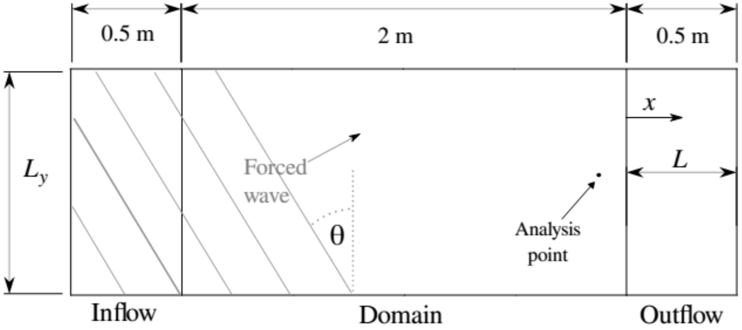

(Ref : Richards 2004, Gill 2015)

Investigated configuration

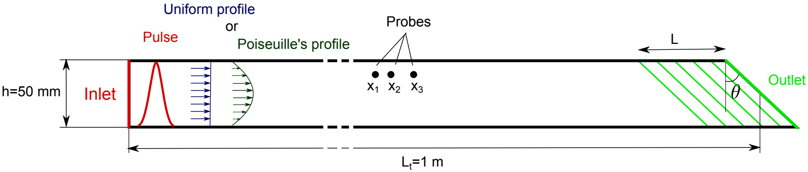

- Two-dimensional channel (length of 1 m, a height of 50 mm, mesh size of 0.25 mm.).
- A gaussian pulse can be imposed at the inlet in addition to an uniform or non-uniform flow.
- The non-reflective boundary condition is set at the outlet with an angle θ and a depth L for buffer zone technique.
- A three-points array is placed around the center of the channel.

Investigated configuration

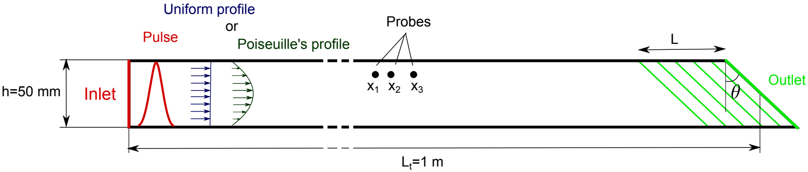

- Two-dimensional channel (length of 1 m, a height of 50 mm, mesh size of 0.25 mm.).
- A gaussian pulse can be imposed at the inlet in addition to an uniform or non-uniform flow.
- The non-reflective boundary condition is set at the outlet with an angle θ and a depth L for buffer zone technique.
- A three-points array is placed around the center of the channel.

Investigated configuration

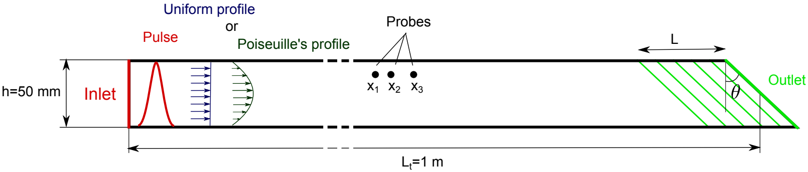

- Two-dimensional channel (length of 1 m, a height of 50 mm, mesh size of 0.25 mm.).
- A gaussian pulse can be imposed at the inlet in addition to an uniform or non-uniform flow.
- The non-reflective boundary condition is set at the outlet with an angle θ and a depth L for buffer zone technique.
- A three-points array is placed around the center of the channel.

Investigated configuration

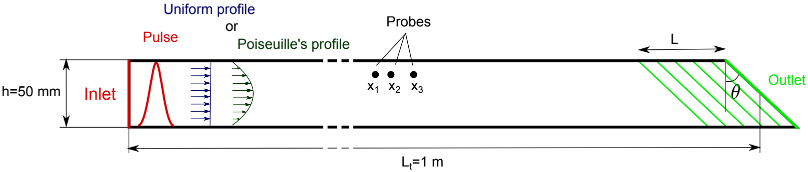

- Two-dimensional channel (length of 1 m, a height of 50 mm, mesh size of 0.25 mm.).
- A gaussian pulse can be imposed at the inlet in addition to an uniform or non-uniform flow.
- The non-reflective boundary condition is set at the outlet with an angle θ and a depth L for buffer zone technique.
- A three-points array is placed around the center of the channel.

Evaluation of the non-reflective conditions in the frequency domain

- The pressure p, solution of the convected Helmhotz equation, can be written as :

$$p\,(x,t) = Ae^{j(\omega t-\beta^{+}x)} + Be^{j(\omega t+\beta^{-}x)} \tag{2}$$

with $\beta^{+} = \dfrac{k_0}{1+M}$, $\beta^{-} = \dfrac{k_0}{1-M}$, $\omega = 2\pi f$ the pulsation, f the frequency, $M = V_0/c_0$ the Mach number, V_0 the mean flow velocity, c_0 the speed of sound and $k_0 = \omega/c_0$ the acoustical wavenumber.

- Knowing the pressure at **two points** x_1 and x_2 and using the **Fourier's transform** enables to calculate the amplitudes of the upstream wave A and the downstream wave B in the frequency domain.

Evaluation of the non-reflective conditions in the frequency domain

- The pressure p, solution of the convected Helmhotz equation, can be written as :

$$p\,(x,t) = Ae^{j(\omega t - \beta^+ x)} + Be^{j(\omega t + \beta^- x)} \tag{2}$$

  with $\beta^+ = \dfrac{k_0}{1+M}$, $\beta^- = \dfrac{k_0}{1-M}$, $\omega = 2\pi f$ the pulsation, f the frequency, $M = V_0/c_0$ the Mach number, V_0 the mean flow velocity, c_0 the speed of sound and $k_0 = \omega/c_0$ the acoustical wavenumber.

- Knowing the pressure at **two points** x_1 and x_2 and using the **Fourier's transform** enables to calculate the amplitudes of the upstream wave A and the downstream wave B in the frequency domain.

Evaluation of the non-reflective conditions in the frequency domain

- The pressure p, solution of the convected Helmhotz equation, can be written as :

$$p(x,t) = Ae^{j(\omega t - \beta^+ x)} + Be^{j(\omega t + \beta^- x)} \quad (2)$$

with $\beta^+ = \dfrac{k_0}{1+M}$, $\beta^- = \dfrac{k_0}{1-M}$, $\omega = 2\pi f$ the pulsation, f the frequency, $M = V_0/c_0$ the Mach number, V_0 the mean flow velocity, c_0 the speed of sound and $k_0 = \omega/c_0$ the acoustical wavenumber.

- Knowing the pressure at **two points** x_1 and x_2 and using the **Fourier's transform** enables to calculate the amplitudes of the upstream wave A and the downstream wave B in the frequency domain.

Evaluation of the non-reflective conditions in the frequency domain

$$A(\omega) = \frac{P_1(\omega)\, e^{j\frac{k_0}{1-M}x_2} - P_2(\omega)\, e^{j\frac{k_0}{1-M}x_1}}{2j\,\sin\left(\frac{k_0}{1-M^2}(x_2-x_1)\right)} e^{-j\frac{k_0 M}{1-M^2}(x_1+x_2)}$$

$$B(\omega) = -\frac{P_1(\omega)\, e^{-j\frac{k_0}{1+M}x_2} - P_2(\omega)\, e^{-j\frac{k_0}{1+M}x_1}}{2j\,\sin\left(\frac{k_0}{1-M^2}(x_2-x_1)\right)} e^{-j\frac{k_0 M}{1-M^2}(x_1+x_2)}$$

Previous equations have a singularity due to the term $\sin\left(\frac{k_0}{1-M^2}(x_2-x_1)\right)$.

This singularity can be avoided using a third probe x_3 satisfying $(x_3-x_2) \neq (x_2-x_1)$.

An automatic procedure may be used for weighting solutions and eliminating the singularities.

Evaluation of the non-reflective conditions in the frequency domain

$$A(\omega) = \frac{P_1(\omega)\,\mathrm{e}^{j\frac{k_0}{1-M}x_2} - P_2(\omega)\,\mathrm{e}^{j\frac{k_0}{1-M}x_1}}{2j\,\sin\left(\frac{k_0}{1-M^2}(x_2-x_1)\right)}\mathrm{e}^{-j\frac{k_0 M}{1-M^2}(x_1+x_2)}$$

$$B(\omega) = -\frac{P_1(\omega)\,\mathrm{e}^{-j\frac{k_0}{1+M}x_2} - P_2(\omega)\,\mathrm{e}^{-j\frac{k_0}{1+M}x_1}}{2j\,\sin\left(\frac{k_0}{1-M^2}(x_2-x_1)\right)}\mathrm{e}^{-j\frac{k_0 M}{1-M^2}(x_1+x_2)}$$

Previous equations have a singularity due to the term $\sin\left(\frac{k_0}{1-M^2}(x_2-x_1)\right)$.

This singularity can be avoided using a third probe x_3 satisfying $(x_3-x_2) \neq (x_2-x_1)$.

An automatic procedure may be used for weighting solutions and eliminating the singularities.

Evaluation of the non-reflective conditions in the frequency domain

$$A(\omega) = \frac{P_1(\omega)\,\mathrm{e}^{j\frac{k_0}{1-M}x_2} - P_2(\omega)\,\mathrm{e}^{j\frac{k_0}{1-M}x_1}}{2j\,\sin\left(\frac{k_0}{1-M^2}(x_2-x_1)\right)}\mathrm{e}^{-j\frac{k_0 M}{1-M^2}(x_1+x_2)}$$

$$B(\omega) = -\frac{P_1(\omega)\,\mathrm{e}^{-j\frac{k_0}{1+M}x_2} - P_2(\omega)\,\mathrm{e}^{-j\frac{k_0}{1+M}x_1}}{2j\,\sin\left(\frac{k_0}{1-M^2}(x_2-x_1)\right)}\mathrm{e}^{-j\frac{k_0 M}{1-M^2}(x_1+x_2)}$$

Previous equations have a singularity due to the term $\sin\left(\frac{k_0}{1-M^2}(x_2-x_1)\right)$.

This singularity can be avoided using a third probe x_3 satisfying $(x_3-x_2) \neq (x_2-x_1)$.

An automatic procedure may be used for weighting solutions and eliminating the singularities.

Evaluation of the non-reflective conditions in the frequency domain

$$A(\omega) = \frac{P_1(\omega)\,\mathrm{e}^{j\frac{k_0}{1-M}x_2} - P_2(\omega)\,\mathrm{e}^{j\frac{k_0}{1-M}x_1}}{2j\,\sin\left(\frac{k_0}{1-M^2}(x_2-x_1)\right)}\mathrm{e}^{-j\frac{k_0 M}{1-M^2}(x_1+x_2)}$$

$$B(\omega) = -\frac{P_1(\omega)\,\mathrm{e}^{-j\frac{k_0}{1+M}x_2} - P_2(\omega)\,\mathrm{e}^{-j\frac{k_0}{1+M}x_1}}{2j\,\sin\left(\frac{k_0}{1-M^2}(x_2-x_1)\right)}\mathrm{e}^{-j\frac{k_0 M}{1-M^2}(x_1+x_2)}$$

Previous equations have a singularity due to the term $\sin\left(\frac{k_0}{1-M^2}(x_2-x_1)\right)$.

This singularity can be avoided using a third probe x_3 satisfying $(x_3-x_2) \neq (x_2-x_1)$.

An automatic procedure may be used for weighting solutions and eliminating the singularities.

Evaluation of the non-reflective conditions in the frequency domain

The reflexion coefficient $R(\omega)$ writes

$$R(\omega) = \frac{B(\omega)}{A(\omega)}$$

and the absorption coefficient is

$$\alpha(\omega) = 1 - |R(\omega)|^2.$$

Pulse excitation

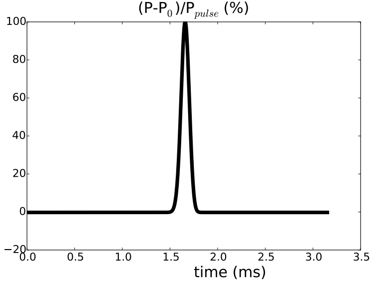

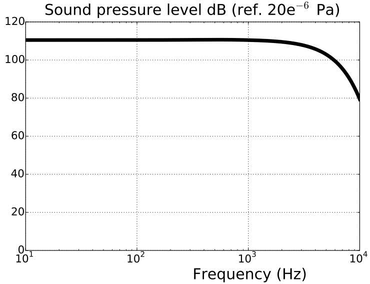

2D-channel without flow

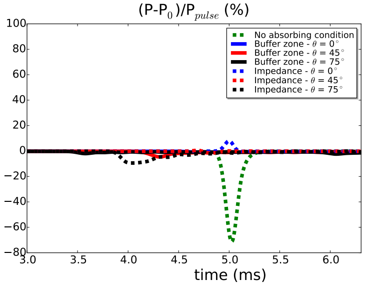

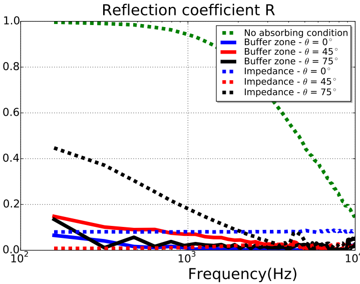

- The reflected pulse is always lower than 5 % with the buffer zone damping and lower than 10 % with the surface impedance.
- The reflection coefficient increases with the incident angle for the surface impedance.
- The damping buffer zone seems relatively robust (even with $\theta = 75°$).

2D-channel without flow

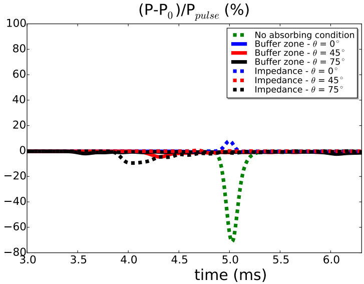

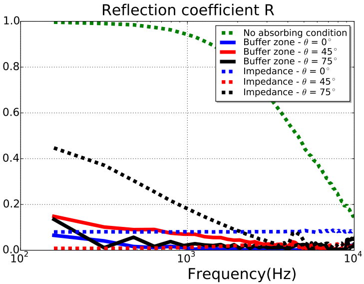

- The reflected pulse is always lower than 5 % with the buffer zone damping and lower than 10 % with the surface impedance.
- The reflection coefficient increases with the incident angle for the surface impedance.
- The damping buffer zone seems relatively robust (even with $\theta = 75°$).

2D-channel without flow

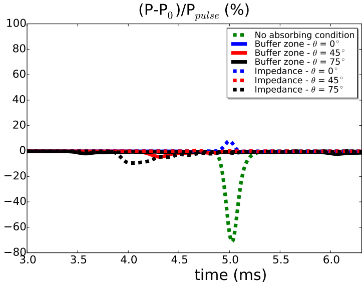

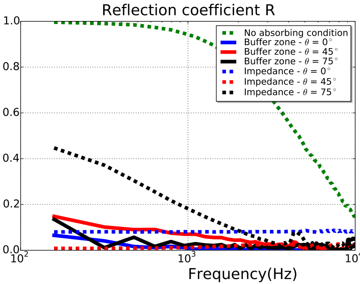

- The reflected pulse is always lower than 5 % with the buffer zone damping and lower than 10 % with the surface impedance.
- The reflection coefficient increases with the incident angle for the surface impedance.
- The damping buffer zone seems relatively robust (even with $\theta = 75°$).

2D-channel without flow

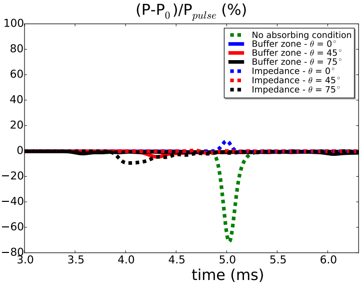

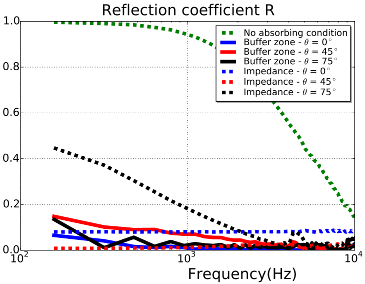

- The reflected pulse is always lower than 5 % with the buffer zone damping and lower than 10 % with the surface impedance.
- The reflection coefficient increases with the incident angle for the surface impedance.
- The damping buffer zone seems relatively robust (even with $\theta = 75^\circ$).

2D-channel with uniform flow

- $V = 100$ m.s^{-1}, $\theta = 0$ or $75°$,
- Target fields are known.

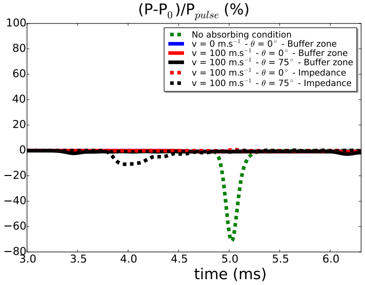

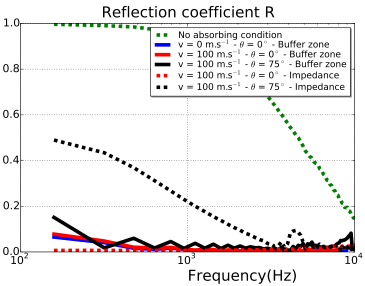

2D-channel with uniform flow

- Residual velocity $V - V_0$ as a percentage of V_{pulse} :

2D-channel with non-uniform flow

- Poiseuille's profile. Target velocities are unknown.

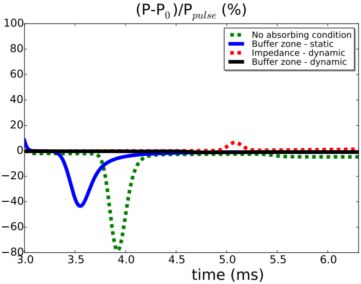

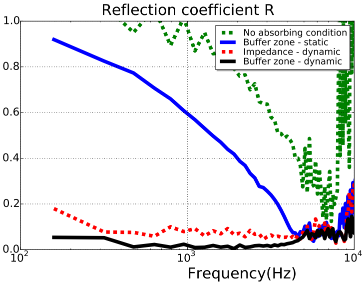

- The static buffer zone method is not able to achieve a good non-reflective condition.
- The use of the dynamic method largely improves the buffer zone damping technique.

2D-channel with non-uniform flow

- Poiseuille's profile. Target velocities are unknown.

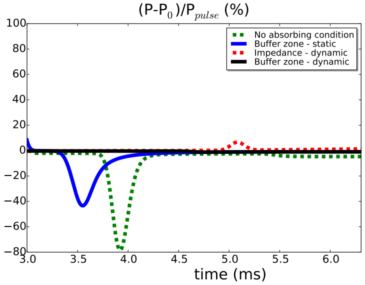

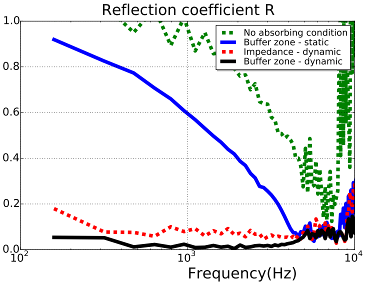

- The static buffer zone method is not able to achieve a good non-reflective condition.
- The use of the dynamic method largely improves the buffer zone damping technique.

2D-channel with non-uniform flow

- Poiseuille's profile. Target velocities are unknown.

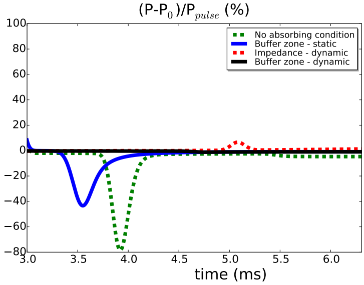

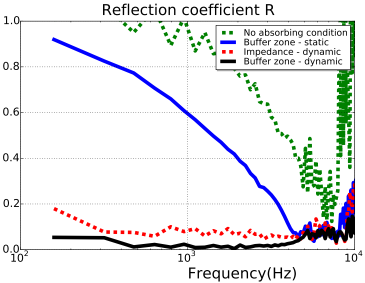

- The static buffer zone method is not able to achieve a good non-reflective condition.
- The use of the dynamic method largely improves the buffer zone damping technique.

2D-channel with non-uniform flow

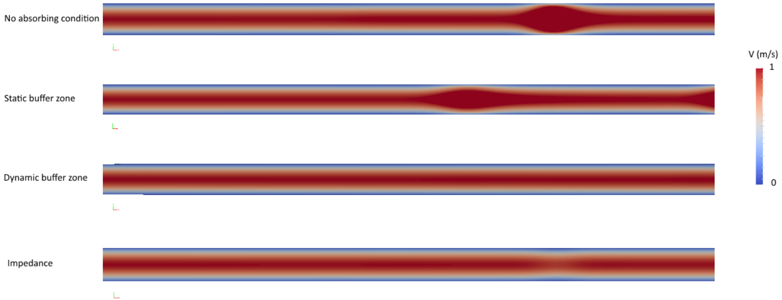

Perspectives for industrial applications

- The configuration of interest is a full scale aircraft standing on the ground where cross-winds induced forces are studied.
- 320 million cells in a computational domain of 400m x 300m x 170m.
- The sponge zone influence has been investigated in terms of the :
  - Ability to damp outgoing acoustic waves efficiently and thus avoid spurious standing waves in the domain.
  - Ability to pass transient time faster.
  - Ability to avoid undesired phenomena such as drift of the mean flow.
- Four computations are carried out : static and dynamic zones of thicknesses 10 and 30 m.

Perspectives for industrial applications

- The configuration of interest is a full scale aircraft standing on the ground where cross-winds induced forces are studied.
- 320 million cells in a computational domain of 400m x 300m x 170m.
- The sponge zone influence has been investigated in terms of the :
  - Ability to damp outgoing acoustic waves efficiently and thus avoid spurious standing waves in the domain.
  - Ability to pass transient time faster.
  - Ability to avoid undesired phenomena such as drift of the mean flow.
- Four computations are carried out : static and dynamic zones of thicknesses 10 and 30 m.

Perspectives for industrial applications

- The configuration of interest is a full scale aircraft standing on the ground where cross-winds induced forces are studied.
- 320 million cells in a computational domain of 400m x 300m x 170m.
- The sponge zone influence has been investigated in terms of the :
  - Ability to damp outgoing acoustic waves efficiently and thus avoid spurious standing waves in the domain.
  - Ability to pass transient time faster.
  - Ability to avoid undesired phenomena such as drift of the mean flow.
- Four computations are carried out : static and dynamic zones of thicknesses 10 and 30 m.

Perspectives for industrial applications

- The configuration of interest is a full scale aircraft standing on the ground where cross-winds induced forces are studied.
- 320 million cells in a computational domain of 400m x 300m x 170m.
- The sponge zone influence has been investigated in terms of the :
  - Ability to damp outgoing acoustic waves efficiently and thus avoid spurious standing waves in the domain.
  - Ability to pass transient time faster.
  - Ability to avoid undesired phenomena such as drift of the mean flow.
- Four computations are carried out : static and dynamic zones of thicknesses 10 and 30 m.

Perspectives for industrial applications

- Integrated forces (along x-component) :

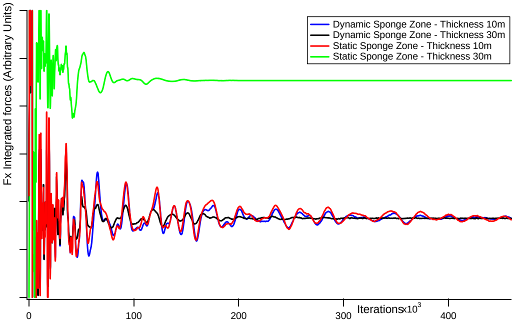

- Converge much faster with a thicker sponge zone.
- A significant drift occurs with the 30-m-thick static sponge zone.
- The 30-m-thick dynamic sponge zone does not yield any drift and yet preserves a fast convergence.

Perspectives for industrial applications

- Integrated forces (along x-component) :

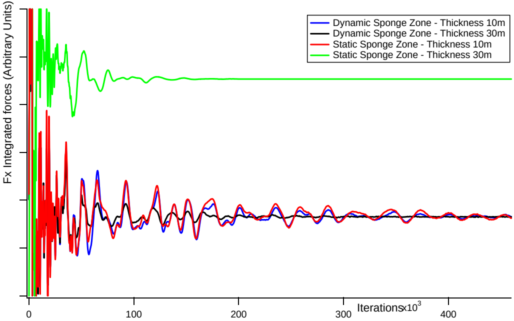

- Converge much faster with a thicker sponge zone.
- A significant drift occurs with the 30-m-thick static sponge zone.
- The 30-m-thick dynamic sponge zone does not yield any drift and yet preserves a fast convergence.

Perspectives for industrial applications

- Integrated forces (along x-component) :

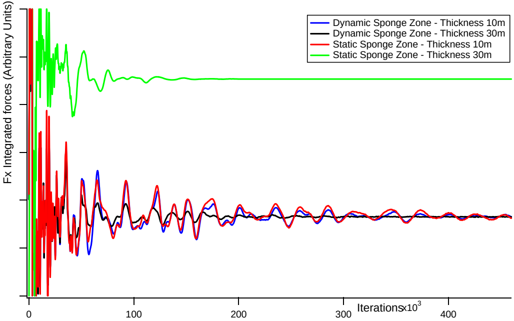

- Converge much faster with a thicker sponge zone.
- A significant drift occurs with the 30-m-thick static sponge zone.
- The 30-m-thick dynamic sponge zone does not yield any drift and yet preserves a fast convergence.

Perspectives for industrial applications

- Integrated forces (along x-component) :

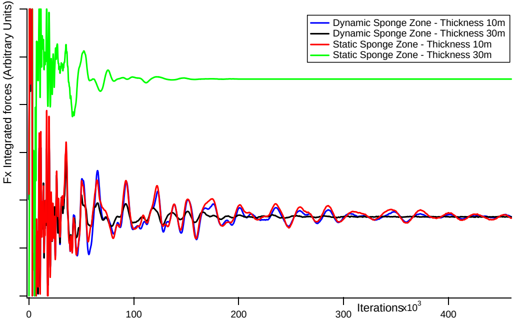

- Converge much faster with a thicker sponge zone.
- A significant drift occurs with the 30-m-thick static sponge zone.
- The 30-m-thick dynamic sponge zone does not yield any drift and yet preserves a fast convergence.

Perspectives for industrial applications

Comparison of the mean velocity magnitude in the symmetry plane Y=0 :

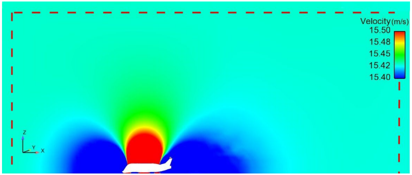

10-m-thick **static** sponge zones

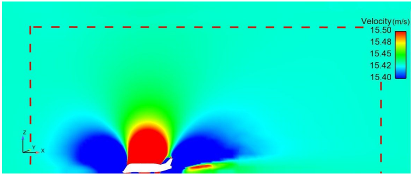

30-m-thick **static** sponge zones

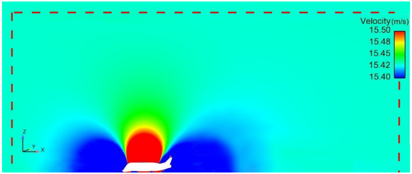

10-m-thick **dynamic** sponge zones

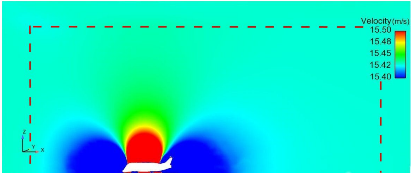

30-m-thick **dynamic** sponge zones

Conclusion

- Two methods achieving non-reflective boundary conditions have been studied in a lattice Boltzmann framework.
- The well known buffer zone damping technique has been compared to the surface impedance method, usually used for acoustic purposes.
- A **simple method to estimate the target field, when unknown**, from a simple accumulator has been introduced.
- A new test case has been used and the analysis of the reflection coefficient has been carried out in **the frequency domain**.
- The methods have been compared for various incident angle and various mean flow configurations (without flow, with uniform and non-uniform flows.).

Conclusion

- Two methods achieving non-reflective boundary conditions have been studied in a lattice Boltzmann framework.
- The well known buffer zone damping technique has been compared to the surface impedance method, usually used for acoustic purposes.
- A **simple method to estimate the target field, when unknown**, from a simple accumulator has been introduced.
- A new test case has been used and the analysis of the reflection coefficient has been carried out in **the frequency domain**.
- The methods have been compared for various incident angle and various mean flow configurations (without flow, with uniform and non-uniform flows.).

Conclusion

- Two methods achieving non-reflective boundary conditions have been studied in a lattice Boltzmann framework.
- The well known buffer zone damping technique has been compared to the surface impedance method, usually used for acoustic purposes.
- A **simple method to estimate the target field, when unknown**, from a simple accumulator has been introduced.
- A new test case has been used and the analysis of the reflection coefficient has been carried out in **the frequency domain**.
- The methods have been compared for various incident angle and various mean flow configurations (without flow, with uniform and non-uniform flows.).

Conclusion

- Two methods achieving non-reflective boundary conditions have been studied in a lattice Boltzmann framework.
- The well known buffer zone damping technique has been compared to the surface impedance method, usually used for acoustic purposes.
- A **simple method to estimate the target field, when unknown**, from a simple accumulator has been introduced.
- A new test case has been used and the analysis of the reflection coefficient has been carried out in **the frequency domain**.
- The methods have been compared for various incident angle and various mean flow configurations (without flow, with uniform and non-uniform flows.).

Conclusion

- Two methods achieving non-reflective boundary conditions have been studied in a lattice Boltzmann framework.
- The well known buffer zone damping technique has been compared to the surface impedance method, usually used for acoustic purposes.
- A **simple method to estimate the target field, when unknown**, from a simple accumulator has been introduced.
- A new test case has been used and the analysis of the reflection coefficient has been carried out in **the frequency domain**.
- The methods have been compared for various incident angle and various mean flow configurations (without flow, with uniform and non-uniform flows.).

Conclusion

- The dynamic sponge zones have been successfully used on an industrial application where the static sponge zones imply a drift on the simulated fields.
- One of the strengths of the current LBM approach lies in the efficiency to go from theoretical modelling stage to realistic application testing in a very straightforward manner.
- The future works should extend and evaluate the characteristic boundary conditions, known to be more efficient than the buffer zone damping method, by using the lattice Boltzmann method and the frequency domain analysis.

Conclusion

- The dynamic sponge zones have been successfully used on an industrial application where the static sponge zones imply a drift on the simulated fields.
- One of the strengths of the current LBM approach lies in the efficiency to go from theoretical modelling stage to realistic application testing in a very straightforward manner.
- The future works should extend and evaluate the characteristic boundary conditions, known to be more efficient than the buffer zone damping method, by using the lattice Boltzmann method and the frequency domain analysis.

Conclusion

- The dynamic sponge zones have been successfully used on an industrial application where the static sponge zones imply a drift on the simulated fields.
- One of the strengths of the current LBM approach lies in the efficiency to go from theoretical modelling stage to realistic application testing in a very straightforward manner.
- The future works should extend and evaluate the characteristic boundary conditions, known to be more efficient than the buffer zone damping method, by using the lattice Boltzmann method and the frequency domain analysis.

Acknowledgments

The authors want to thank A. Sengissen and T. Astoul from Airbus Operations SAS for the computation on the industrial case and their useful comments.

B. Gaston & R. Cuidard from CS are greatly acknowledged for their support on Lattice Boltzmann Solver.

Present work has been supported by French funded projects LABS & CLIMB in the frame of the "Programme d'Investissement d'Avenir : Calcul Intensif et Simulation Numérique".

Conclusion

Thank You For Your Attention !